Solvent-Free Oxidation of Primary Alcohols to Aldehydes Using Au-Pd/TiO 2 Catalysts

Dan I. Enache, *et al.*

Science **311**, 362 (2006);
DOI: 10.1126/science.1120560

Solvent-Free Oxidation of Primary Alcohols to Aldehydes Using Au-Pd/TiO_2 Catalysts

Dan I. Enache,[1] Jennifer K. Edwards,[1] Philip Landon,[1] Benjamin Solsona-Espriu,[1] Albert F. Carley,[1] Andrew A. Herzing,[2] Masashi Watanabe,[2] Christopher J. Kiely,[2] David W. Knight,[1] Graham J. Hutchings[1]*

The oxidation of alcohols to aldehydes with O_2 in place of stoichiometric oxygen donors is a crucial process for the synthesis of fine chemicals. However, the catalysts that have been identified so far are relatively inactive with primary alkyl alcohols. We showed that Au/Pd-TiO_2 catalysts give very high turnover frequencies (up to 270,000 turnovers per hour) for the oxidation of alcohols, including primary alkyl alcohols. The addition of Au to Pd nanocrystals improved the overall selectivity and, using scanning transmission electron microscopy combined with x-ray photoelectron spectroscopy, we showed that the Au-Pd nanocrystals were made up of a Au-rich core with a Pd-rich shell, indicating that the Au electronically influences the catalytic properties of Pd.

Selective oxidation is important in the synthesis of fine chemicals and intermediates (*1*); and, in particular, the oxidation of primary alcohols to aldehydes is a fundamentally important laboratory and commercial procedure (*1*–*8*). Aldehydes are valuable both as intermediates and as high-value components for the perfume industry (*1*, *9*, *10*). Many oxidations of this type are carried out using stoichiometric oxygen donors such as chromate or permanganate, but these reagents are expensive and have serious toxicity issues associated with them (*1*, *9*, *11*–*14*). In many cases, aldehydes are obtained only from activated alcohols in which the carbon bears a phenyl group, such as benzyl alcohol (*7*, *8*). Sheldon and co-workers (*3*) have obtained good yields from a biphasic system for the catalytic conversion of pentan-1-ol to the aldehyde, but the acid is produced in the case of hexan-1-ol. Given these limitations, there is substantial interest in the development of heterogeneous catalysts that use either O_2 or H_2O_2 as the oxidant (*15*). Au nanocrystals have been shown to be highly effective for the oxidation of alcohols with O_2 in an aqueous base, in particular diols and triols; but under these conditions, the product is the corresponding monoacid, not the aldehyde (*16*–*19*). Gold catalysts have, however, been found to be effective for the gas-phase oxidation of volatile alcohols to the corresponding aldehydes and ketones (*20*).

Most recently, two studies have shown that supported metal nanoparticles can be very effective catalysts for the oxidation of alcohols to aldehydes, using O_2 under relatively mild conditions. Kaneda and co-workers (*6*) found that hydroxyapatite-supported Pd nanoclusters (Pd/HAP) give very high turnover frequencies (TOFs) for the oxidation of phenylethanol and benzyl alcohol but show limited activity for the oxidation of primary alkyl alcohols (such as octan-1-ol oxidation). Corma and co-workers (*21*) have shown that the addition of Au nanocrystals to CeO_2 converts the oxide from a stoichiometric oxidant to a catalytic system, with TOFs similar to those obtained by Kaneda and co-workers (*6*).

Recently, we have shown that supported Au-Pd alloys are efficient catalysts for the direct synthesis of H_2O_2 from H_2 oxidation by O_2 at low temperatures (*22*–*25*). In particular, Au-Pd/TiO_2 catalysts were very selective for H_2O_2 synthesis. Hydroperoxy species are considered to be involved in this H_2O_2 formation process, and because hydroperoxy species are key reagents/intermediates in the oxidation of alcohols (*1*), we reasoned that these catalysts should also be effective for the oxidation of alcohols. We showed that TiO_2-supported Au-Pd alloy nanocrystals give significantly enhanced activity for alcohol oxidation using a green chemistry approach with O_2 under mild solvent-free conditions. When compared with monometallic supported Au (*21*) and Pd (*6*), the Au-Pd catalysts nanocrystals give TOFs that are enhanced by a factor of ~25.

The TiO_2-supported Au-Pd catalysts were initially investigated for the oxidation of benzyl alcohol at 373 K with O_2 as oxidant in the absence of solvent (Fig. 1A). The Au-Pd/TiO_2 catalysts were very active for this reaction, and the selectivity to benzaldehyde was ≥96%, with the only byproduct being benzyl benzoate. In contrast, Pd/TiO_2 also produced toluene and benzene as byproducts, and a Au/TiO_2 catalyst produced a significant amount of an acetal product. The selectivity of the Au/TiO_2 catalyst for benzaldehyde decreased with the time on line, but further oxidation of the acetal byproduct led to an increase of the final selectivity in benzaldehyde. Carbon mass balances were 100%, and no carbon oxides were formed for Au-Pd/TiO_2 or Au/TiO_2 catalysts.

The effect of adding Au to a Pd/TiO_2 catalyst is apparent in these initial studies. Al-

[1]School of Chemistry, Cardiff University, Main Building, Park Place, Cardiff, UK CF10 3AT. [2]Center for Advanced Materials and Nanotechnology, Lehigh University, 5 East Packer Avenue, Bethlehem, PA 18015–3195, USA.

*To whom correspondence should be addressed. E-mail: hutch@cf.ac.uk

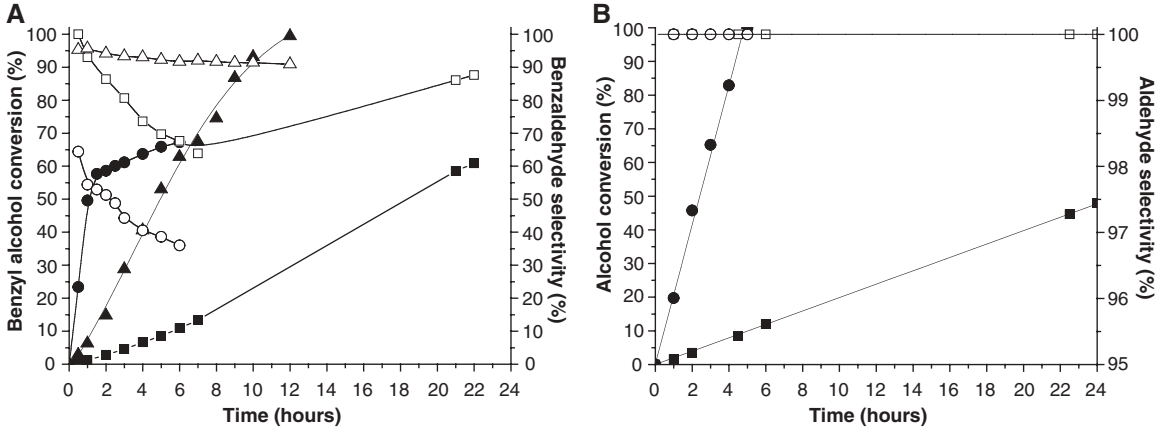

Fig. 1. (**A**) Benzyl alcohol conversion and selectivity in benzaldehyde with the reaction time at 373 K and 0.1 MPa pO_2. Squares, Au/TiO_2; circles, Pd/TiO_2; and triangles, Au-Pd/TiO_2. Solid symbols indicate conversion, and open symbols indicate selectivity. (**B**) Au-Pd/TiO_2 catalyzed reactions at 363 K, 0.1 MPa pO_2, for cinnamyl alcohol (squares) and vanillyl alcohol (circles). Solid symbols indicate conversion, and open symbols indicate selectivity to the corresponding aldehydes.

though the Pd/TiO_2 catalyst has a high initial activity, and the addition of Au decreases the activity, the $Au-Pd/TiO_2$ catalyst retained high selectivity to benzaldehyde at high conversion rates, a feature not observed with the supported pure-Au and pure-Pd catalysts. One of the key factors that must be considered for heterogeneous catalysts operating in three-phase systems is the possibility that active components can leach into the reaction mixture, thereby leading to catalyst deactivation or, in the worst case, to the formation of an active homogeneous catalyst. We have found that the catalysts calcined at 673 K are stable and do not leach Au or Pd into solution, a feature we have previously also observed in our studies on hydrogen peroxide synthesis (*24*, *25*) (see supporting online material).

Because Al_2O_3 and Fe_2O_3 were also effective supports for the formation of H_2O_2 with Au-Pd nanocrystals, these catalysts were also investigated, but the TiO_2-supported Au-Pd catalysts are preferred for the oxidation of benzyl alcohol (Table 1); it is likely that the more acidic nature of the Al_2O_3 and Fe_2O_3 supports led to enhanced byproduct formation.

The $Au-Pd/TiO_2$ catalysts were investigated with a range of substrates and conditions (Table 2). In the initial experiments conducted at 373 K (Table 2, entries 1 to 3), relatively high catalyst loadings were used, but selectivities >90% could still be achieved for the oxidation of benzyl alcohol to benzaldehyde. Subsequent experiments used much lower metal concentrations, and the effect of the pressure of O_2 (pO_2) (Table 2, entries 4 to 7) showed that the reaction was of zero order in O_2. The selectivity to the aldehydes increased with pO_2 [for conversions of benzyl alcohol, >70%, the selectivity to the aldehyde increased from 71% at low pO_2 (Table 2, entry 4) to 86% at the higher pO_2 (Table 2, entry 6)] and metal concentration, but selectivities of >80% were achieved readily under most conditions. These initial experiments were conducted in a closed autoclave with O_2 at a constant reaction pressure, so that as the reaction proceeded and O_2 was consumed, this oxygen was replenished. We have used air in place of O_2 and have obtained the same initial TOFs, which demonstrates that in principle, air can be used for industrial applications. Increasing the temperature (Table 2, entries 4 and 8 to 10) increased the rate as expected (with activation energy E_A = 45.8 kJ/mol), but the selectivity decreased to ~60% at 433 K, and the byproducts included benzylbenzoate and toluene under these more forcing conditions. The $Au-Pd/TiO_2$ catalysts were very active, and the best performance (Fig. 1A) was achieved at lower temperatures (≤373 K), higher pO_2 (0.2 to 1.0 MPa), and higher catalyst loadings, but we stress that we have

Table 1. Comparative data for benzyl alcohol oxidation and hydrogen peroxide synthesis. Results were obtained for the oxidation of benzyl alcohol after 0.5 hour and 8 hours of reaction and for H_2O_2 synthesis for 0.5 hour. The oxidation of benzyl alcohol was carried out at 373 K temperature, 0.2 MPa pO_2, and 1500 rpm stirrer speed. The H_2O_2 synthesis was carried out under the conditions described in (*26*, *27*). Productivities are quoted in units of moles of product per hour per kilogram of catalyst.

Catalyst	Benzyl alcohol oxidation					H_2O_2 productivity [mol/(hour/kg_{cat})]
	Conversion (%)		Benzaldehyde selectivity (%)		Benzaldehyde productivity* [mol/(hour/kg_{cat})]	
	0.5 hour	8 hours	0.5 hour	8 hours		
2.5% Au–2.5% Pd/Al_2O_3	2.6	83.3	90.5	86.6	174	23
2.5% Au–2.5% Pd/TiO_2	3.7	74.5	95.2	91.6	165	64
2.5% Au–2.5% Pd/SiO_2	3.6	35.7	97.3	88.0	76	80
2.5% Au–2.5% Pd/Fe_2O_3	3.6	63.4	74.9	66.4	102	16
2.5% Au–2.5% Pd/C	2.9	69.2	53.9	46.4	78	30
2.5% Au/TiO_2	0.6	15.3	96.7	63.9	24	<2
2.5% Pd/TiO_2	13.4	60.1	51.3	54.4	79	24

*Calculated for 8 hours of reaction.

Table 2. Comparison of the catalytic activity for alcohol oxidation to the corresponding aldehyde. Catalyst is 2.5% Au–2.5% Pd/TiO_2 unless noted otherwise; substrates oxidized without solvent unless specified; catalyst mass varied to give the metal concentrations indicated; and TOF was measured after first 0.5 hour of reaction. *T*, temperature.

Entry	Alcohol	Reaction conditions		[Metal] (10^{-5} mol/liter)		TOF (/hour)
		T (K)	*P* (10^5 Pa)	Au	Pd	
1	Benzyl alcohol	373	2	63.5	118	607
2	Benzyl alcohol*	373	2	63.5	0	213
3	Benzyl alcohol†	373	2	0	118	2,200
4	Benzyl alcohol	373	1	2.1	3.9	6,190
5	Benzyl alcohol	373	2	2.1	3.9	6,440
6	Benzyl alcohol	373	5	2.1	3.9	6,190
7	Benzyl alcohol	373	10	2.1	3.9	5,950
8	Benzyl alcohol	383	1	2.1	3.9	14,270
9	Benzyl alcohol	393	1	2.1	3.9	26,400
10	Benzyl alcohol	433	1	2.1	3.9	86,500
11	1-Phenylethanol	433	1	1.8	3.2	269,000
12	3-Phenyl-1-propanol	433	1	2.1	3.9	2,356
13	Vanillyl alcohol‡	363	1	21.6	40.6	10
14	Cinnamyl alcohol§	363	1	21.6	40.6	97
15	Octan-1-ol	433	1	2.5	4.7	2,000
16	Octan-2-ol	433	1	2.5	4.7	0
17	Octan-2-ol/octan-1-ol	433	1	2.1	3.9	0
18	Octan-3-ol	433	1	2.1	3.9	10,630
19	1-Octen-3-ol	433	1	2.1	3.9	12,600
20	Crotyl alcohol	433	5	2.1	3.9	12,600
21	Butan-1-ol	433	5	2.1	3.9	5,930
22	1,2-Butanediol	433	1	2.1	3.9	1,520
23	1,4-Butanediol	433	1	2.1	3.9	104,200
24	Benzyl alcohol‖	433	1	2.1	3.9	12,500
25	Benzyl alcohol¶	433	1	2.1	0	12,400
26	Benzyl alcohol#	433	1	0	3.9	24,800
27	Benzyl alcohol**	433	1	2.4	4.5	36,500
28	Benzyl alcohol††	433	1	0	3.6	37,600
29	1-Phenylethanol††	433	1	0	3.1	11,600

*2.5% Au/TiO_2. †2.5% Pd/TiO_2. ‡0.2 mol/liter in toluene as solvent. §0.2 mol/liter in water as solvent. ‖2.5% Au–2.5% Pd/HAP prepared by impregnation of HAP with $HAuCl_4{\cdot}3H_2O$ and $PdCl_2$. ¶2.5% Au/HAP prepared by impregnation of HAP with $HAuCl_4{\cdot}3H_2O$. #2.5% Pd/HAP prepared by impregnation of HAP with $PdCl_2$. **2.5% Au–2.5% Pd/TiO_2 prepared with the method of Kaneda (*6*) using TiO_2 as support. ††0.2% Pd/HAP prepared using the method of Kaneda (*6*) using HAP as support.

not attempted to optimize the performance at this time. Vanillyl alcohol and cinnamyl alcohol, two important aromatic unsaturated alcohols, were oxidized in the presence of solvents, and 100% specificity to the aldehydes was achieved in both cases at 363 K, further confirming the efficacy of these supported mixed-metal catalysts (Table 2, entries 13 and 14, and Fig. 1B).

As noted above, both Kaneda and co-workers (*6*) and Corma and co-workers (*21*) have shown that supported Pd and Au monometallic catalysts are highly effective for the oxidation of 1-phenylethanol under solvent-free conditions at 433 K with a pO_2 of 0.1 MPa. Under these conditions, the Pd/HAP and Au/CeO_2 catalysts gave TOFs of 9800 and 12,500/hour for 1-phenylethanol, and we have replicated the results for the Pd/HAP catalyst (Table 2, entries 28 and 29). With our $Au\text{-}Pd/TiO_2$ catalyst, we obtained a TOF of 269,000/hour. The $Au\text{-}Pd/TiO_2$ catalyst is also effective for a range of straight-chain, benzylic, and unsaturated alcohols (Table 2, entries 12 to 23) and, in particular, for the oxidation of primary alcohols, such as butan-1-ol and octan-1-ol (Table 2, entries 15 and 21), and high TOFs are observed. This trend was also observed with 1,4-butanediol, for which the observed reactivity is significantly enhanced over that observed for butan-1-ol. This difference may be due to the interaction of this substrate with the active site (Table 2, entry 23), but 1,2-butanediol is much less active (Table 2, entry 22). Even at high reaction temperatures, octan-2-ol is inactive (Table 2, entries 16 and 17), which is in direct contrast with the Pd/HAP and Au/CeO_2 catalysts, for which secondary alcohols are more reactive than primary alcohols. However, the effect of decreased reactivity appears to be limited to 2-alcohols, because octan-3-ol is very reactive (Table 2, entry 18). The addition of octan-2-ol to a reaction mixture leads to a total loss of activity with our catalyst (Table 2, entry 17), and the addition of octan-2-one in small amounts has a similar effect. These findings may indicate a specific interaction of these ketones with the Au-Pd catalyst. To show that TiO_2 is a particularly effective support, we contrasted catalysts prepared using HAP and TiO_2 as supports with the standard impregnation method we have used (Table 2, entries 10 and 25 to 27); it is clear that the TiO_2 support gives improved activity. There is, however, considerable scope to improve and optimize the performance of these mixed metal Au-Pd catalysts in future studies.

The TiO_2-supported Au-Pd catalyst was characterized using x-ray photoelectron spectroscopy (XPS) and scanning transmission electron microscopy (STEM). The XPS results (Fig. 2A) show that the surfaces of the metal nanoparticles in the calcined catalyst material are significantly enriched with Pd. The uncalcined sample shows XPS signals characteristic of both Au and Pd, but as we have stated earlier, these materials are not stable under the reaction conditions. Once calcined at 673 K, the catalysts are stable, and the signal for Au is significantly decreased. STEM analyses of individual metal nanoparticles in the calcined $Au\text{-}Pd/TiO_2$ catalysts were carried out, such as those presented in the montage of annular dark-field (ADF) images and energy-dispersive x-ray (XEDS) maps in Fig. 2B. The Pd x-ray signal originates from a slightly larger spatial area than that of the corresponding Au x-ray signal. This effect is best illustrated in the color map that overlays the filtered Ti, Pd, and Au x-ray signals after the application of multivariate statistical analysis (*26*). In agreement with the XPS study, we deduce that Pd surface seg-

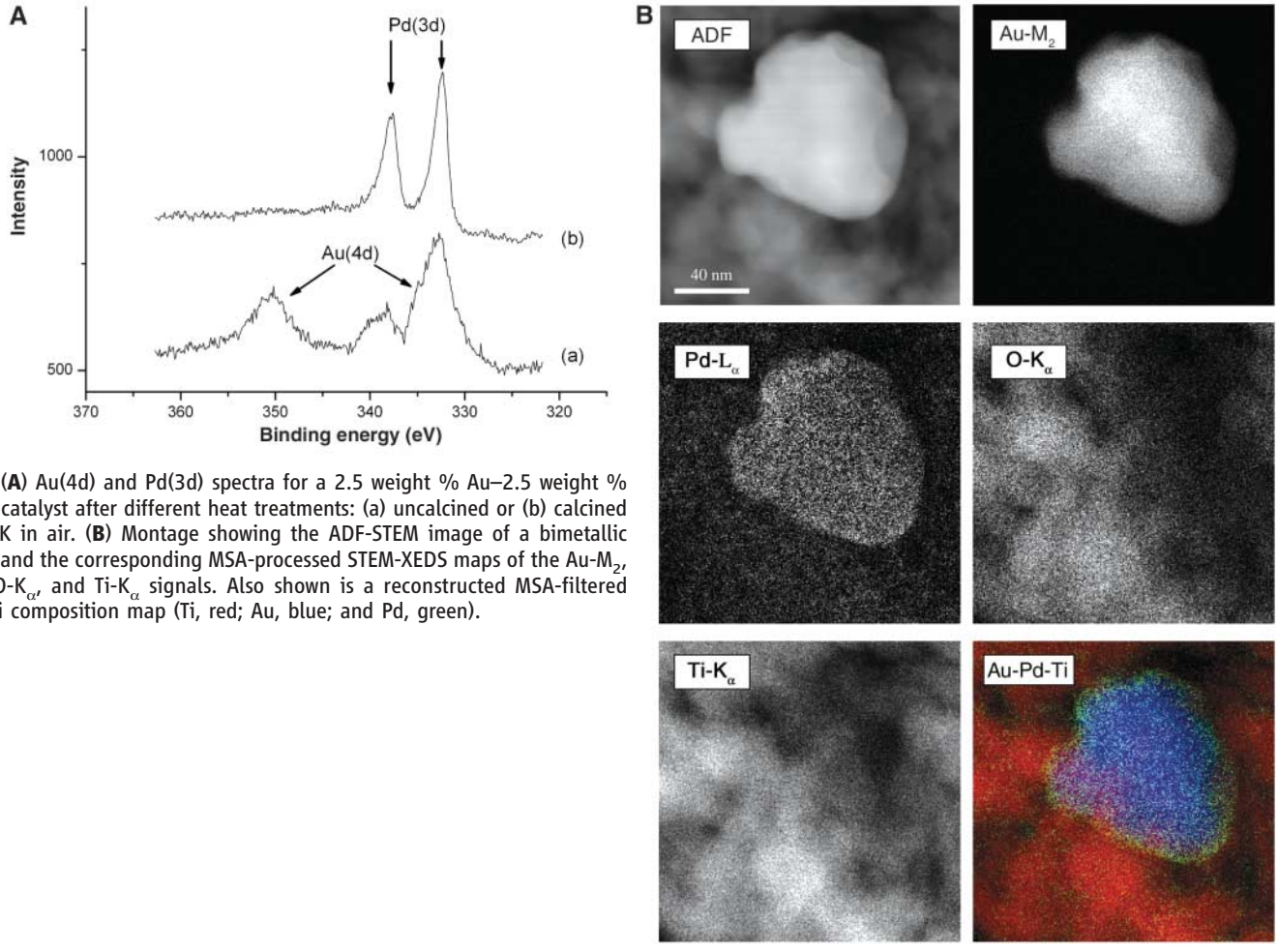

Fig. 2. (**A**) Au(4d) and Pd(3d) spectra for a 2.5 weight % Au–2.5 weight % Pd/TiO_2 catalyst after different heat treatments: (a) uncalcined or (b) calcined at 673 K in air. (**B**) Montage showing the ADF-STEM image of a bimetallic particle and the corresponding MSA-processed STEM-XEDS maps of the $Au\text{-}M_2$, $Pd\text{-}L_\alpha$, $O\text{-}K_\alpha$, and $Ti\text{-}K_\alpha$ signals. Also shown is a reconstructed MSA-filtered Au-Pd-Ti composition map (Ti, red; Au, blue; and Pd, green).

regation occurs during calcination to produce alloy nanoparticles having a Pd-rich shell surrounding a Au-rich core.

The catalytic data show that the introduction of Au to Pd improves selectivity, and we believe that the surface of the bimetallic nanoparticles will still contain some Au. Hence, we argue that the Au acts as an electronic promoter for Pd and that the active catalyst has a surface that is significantly enriched in Pd. Recent studies have started to provide insights into the nature of such effects. For example, Okazaki *et al*. (*27*) have shown, using a combination of experiment and theory, that the electronic structure of Au in Au/TiO_2 catalysts is dependent on the particle size, and Goodman and co-workers (*28*), using model studies, have shown that Au can isolate Pd sites within bimetallic systems.

References and Notes

1. R. A. Sheldon, J. K. Kochi, *Metal-Catalyzed Oxidations of Organic Compounds* (Academic Press, New York, 1981).
2. M. Beller, C. Bolm, *Transition Metals for Organic Synthesis* (Verlag GmbH & Co. KGaA, Weinheim, Germany, ed. 2, 2004).
3. G. ten Brink, I. W. C. E. Arends, R. A. Sheldon, *Science* **287**, 1636 (2000).
4. M. Vazylyev, D. Sloboda-Rozner, A. Haimov, G. Maayan, R. Neumann, *Top. Catal.* **34**, 93 (2005).
5. M. Pagliaro, S. Campestrini, R. Ciriminna, *Chem. Soc. Rev.* **34**, 837 (2005).
6. K. Mori, T. Hara, T. Mizugaki, K. Ebitani, K. Kaneda, *J. Am. Chem. Soc.* **26**, 10657 (2004).
7. I. E. Markó, P. R. Giles, M. Tsukazaki, S. M. Brown, C. J. Urch, *Science* **274**, 2044 (1996).
8. M. J. Schultz, R. S. Adler, W. Zierkiewicz, T. Privalov, M. S. Sigman, *J. Am. Chem. Soc.* **127**, 8499 (2005).
9. U. R. Pillai, E. Sahle-Demessie, *Appl. Catal. Gen.* **245**, 103 (2003).
10. M. Hudlicky, *Oxidations in Organic Chemistry* (American Chemical Society, Washington, DC, 1990).
11. W. P. Griffith, J. M. Joliffe, *Stud. Surf. Sci. Catal.* **66**, 395 (1991).
12. G. Cainelli, G. Cardillo, *Chromium Oxidants in Organic Chemistry* (Springer, Berlin, 1984).
13. D. G. Lee, U. A. Spitzer, *J. Org. Chem.* **35**, 3589 (1970).
14. F. M. Menger, C. Lee, *Tetrahedron Lett.* **22**, 1655 (1981).
15. R. Neumann, M. Levin-Elad, *Appl. Catal. A* **122**, 85 (1995).
16. L. Prati, M. Rossi, *J. Catal.* **176**, 552 (1998).
17. F. Porta, L. Prati, M. Rossi, G. Scari, *J. Catal.* **211**, 464 (2002).
18. S. Carretin, P. McMorn, P. Johnston, K. Griffin, G. J. Hutchings, *Chem. Commun.* **2002**, 696 (2002).
19. F. Porta, L. Prati, *J. Catal.* **224**, 397 (2004).
20. S. Biella, M. Rossi, *Chem. Commun.* **2003**, 378 (2003).
21. A. Abad, P. Conception, A. Corma, H. Garcia, *Angew. Chem.* **44**, 4066 (2005).
22. P. Landon, P. J. Collier, A. J. Papworth, C. J. Kiely, G. J. Hutchings, *Chem. Commun.* **2002**, 2058 (2002).
23. P. Landon *et al.*, *Phys. Chem. Chem. Phys.* **5**, 1917 (2003).
24. J. K. Edwards *et al.*, *J. Mater. Chem.* **15**, 4595 (2005).
25. J. K. Edwards *et al.*, *J. Catal.* **236**, 69 (2005).
26. To confirm that surface segregation of Pd was truly occurring in these nanoparticles, multivariate statistical analysis (MSA) was performed on the data set shown in Fig. 2B. MSA is a group of processing techniques that can be used to identify specific features within large data sets such as x-ray spectrum images and to reduce random noise components in the data sets in a statistical manner. MSA has recently been shown to be particularly useful for analysis of x-ray maps taken from nanoparticles (*29*). This statistical technique performs a data-smoothing calculation by portioning the XEDS data using a probability density function.
27. K. Okazaki, S. Ichikawa, Y. Maeda, M. Haruta, M. Kohyama, *Appl. Catal. A* **291**, 45 (2005).
28. M. Chen, D. Kumar, C.-W. Yi, D. W. Goodman, *Science* **310**, 291 (2005).
29. N. Bonnet, *J. Microsc.* **190**, 2 (1998).

30. Sponsored by the European Union AURICAT project (contract HPRN-CT-2002-00174) and the Engineering and Physical Sciences Research Council (EPSRC) as part of the ATHENA project co-sponsored by Johnson Matthey, as well as by an EPSRC-sponsored program on Speculative Green Chemistry, and we thank them for funding this research. We also thank the World Gold Council (through the GROW scheme) and Cardiff University (AA Reed studentship) for providing support for J.K.E. D.I.E. thanks the Crystal Faraday Partnership for funding. Finally, C.J.K., M.A.W., and A.A.H. gratefully acknowledge NSF funding through the Materials Research Science and Engineering Center (NSF grants DMR-0079996, DMR-0304738, and DMR-0320906).

Supporting Online Material

www.sciencemag.org/cgi/content/full/311/5759/362/DC1
Materials and Methods
Fig. S1

26 September 2005; accepted 7 December 2005
10.1126/science.1120560

Internal Rotation and Spin Conversion of CH_3OH in Solid para-Hydrogen

Yuan-Pern Lee,[1,2]* Yu-Jong Wu,[3] R. M. Lees,[4] Li-Hong Xu,[4] Jon T. Hougen[5]

The quantum solid para-hydrogen (p-H_2) has recently proven useful in matrix isolation spectroscopy. Spectral lines of compounds embedded in this host are unusually narrow, and several species have been reported to rotate in p-H_2. We found that a p-H_2 matrix inhibits rotation of isolated methanol (CH_3OH) but still allows internal rotation about the C–O bond, with splittings of the *E*/*A* torsional doublet in internal rotation–coupled vibrational modes that are qualitatively consistent with those for CH_3OH in the gaseous phase. This simplified high-resolution spectrum further revealed the slow conversion of nuclear spin symmetry from species *E* to species *A* in the host matrix, offering potential insight into nuclear spin conversion in astrophysical sources.

In a quantum solid, the de Broglie wavelength of the species with small mass becomes a substantial fraction of its size at low temperature, resulting in delocalization of the nuclei. Because of the "softness" associated with the quantum solid properties of a p-H_2 matrix (*1*–*3*), guest molecules such as methane can rotate in solid p-H_2 more readily than in other matrices; the rotational parameters of species isolated in p-H_2 are typically ~90% of those for the gaseous phase, even less affected than the parameters of species in helium droplets (*4*, *5*). For larger species, molecular rotation is less likely to occur but internal rotation (torsion) of methyl groups could well persist.

The torsional motion itself is one representative of the class of large-amplitude molecular vibrational motions. In common with overall rotation, these vibrational motions involve displacements of atoms over distances comparable to chemical bond lengths, but in contrast to rotational motions, they are hindered by potential barriers reflective of some mixture of chemical bond properties and van der Waals repulsions.

Internal rotation typically couples with other vibrational modes to give a substantial variety of energy patterns. This coupling with torsional bath states is also believed to be the mechanism responsible for the large enhancement of intramolecular vibrational energy redistribution rates in methyl rotor–containing molecules. Spectral analysis of vibration-rotation bands involving internal rotation is often challenging, but the low-temperature solid p-H_2 environment ensures that nearly all absorption lines originate from the lowest levels. Moreover, fine structure is observable because the infrared (IR) absorption lines of guest molecules in the p-H_2 matrix can be extremely sharp, with full widths at half maximum (FWHM) less than 0.01 cm^{-1} (*4*, *6*).

Here we apply the advantages of p-H_2 to vibrational spectroscopy of methanol. We have observed torsional tunneling splittings between the *A* and *E* symmetry species associated with internal rotation about the C–O bond, permitting a clear differentiation between the corresponding $I = 3/2$ and $I = ½$ nuclear spin modifications of the methyl hy-

[1]Department of Applied Chemistry and Institute of Molecular Science, National Chiao Tung University, 1001 Ta-Hsueh Road, Hsinchu 30010, Taiwan. [2]Institute of Atomic and Molecular Sciences, Academia Sinica, Taipei 10617, Taiwan. [3]Department of Chemistry, National Tsing Hua University, 101, Sec. 2, Kuang Fu Road, Hsinchu 30013, Taiwan. [4]Centre for Laser, Atomic and Molecular Sciences, Department of Physical Sciences, University of New Brunswick, 100 Tucker Park Road, Saint John, New Brunswick E2L 4L5, Canada. [5]Optical Technology Division, National Institute of Standards and Technology, Gaithersburg, MD 20899, USA.

*To whom correspondence should be addressed. E-mail: yplee@mail.nctu.edu.tw